

## Use of aster images for the detection of iron in the deposits of continental terminal 3 (Ct<sup>3</sup>) in the Arewa region, southwest of the Iullemeden basin in Niger.

Daouda Illia Allo <sup>1,\*</sup>, Karimou Dia Hantchi <sup>1</sup>, Karimou Laouali Idi <sup>2</sup>, Maman Mansour Badamassi Kadri <sup>1</sup>, Abdoulwahid Sani <sup>3</sup> and Abdourazakou Maman Hassan <sup>4</sup>

<sup>1</sup> *André Salifou university, Faculty of Science and Technology, Department of Geology, Zinder, Niger.*

<sup>2</sup> *Abdou Moumouni University, Ecole Normale Supérieure, Department of SVT, Niamey, Niger.*

<sup>3</sup> *University of Agadez, faculty of science and technology, department of geology, Agadez, Niger.*

<sup>4</sup> *School of Mining, Industry and Geology, Department of Geosciences, Niamey- Niger.*

World Journal of Advanced Research and Reviews, 2024, 24(03), 1163–1171

Publication history: Received on 31 October 2024; revised on 11 December 2024; accepted on 13 December 2024

Article DOI: <https://doi.org/10.30574/wjarr.2024.24.3.3740>

### Abstract

The present study was carried out in the south-western part of Niger. The study area corresponds to the Arewa region, which is located in the southwestern part of the Iullemeden basin. The general objective of this work is to highlight the effectiveness of the ASTER image in mapping areas with showings of iron mineralization in the Continental Terminal 3 (Ct<sup>3</sup>) formation. Specifically, these areas are identified with major indices of iron oxides and hydroxides (Fe<sub>2</sub>O<sub>3</sub> – Fe(OH)<sub>2</sub>) and goethite Fe(OH)<sub>3</sub>. The methodology implemented is based on band ratios and indices as well as the Main Component Analysis (PCA) were applied to the ASTER image of the study area and allowed the detection and mapping of anomalies related to the presence of iron in the Continental Terminal 3 formation. The band ratios applied to the bands of the ASTER image were very useful for mapping the distribution of iron in the study area and allowed to differentiate the spatial distribution of ferrous iron (Fe<sup>2+</sup>) and ferric iron (Fe<sup>3+</sup>) in the area. The Band 1/Band 2 and Band 2/Band 1 ratios were used to detect the spatial distribution of ferrous iron (Fe<sup>2+</sup>) and ferric iron (Fe<sup>3+</sup>) of the study area, respectively. The results of the Principal Component Analysis (PCA) were very effective in detecting iron-associated minerals or groups of minerals in the area. The presence of iron oxide is predicted by Aster bands 1, 2 and 4 in CP<sub>3</sub>, which are distinguished by bright pixels. CP<sub>6</sub> reveals negative effects of bands 7 and 8 on Fe(OH)-containing minerals.

**Keywords:** Iullemeden basin; Arewa; Continental terminal; ASTER Image; Iron

### 1. Introduction

The contribution of geomatics associated with other integrated approaches (geophysics and geochemistry) should be studied in depth to adopt and develop a multidisciplinary approach for the prospecting of metal deposits (Abdessamad El Atillah et al 2018). It is in this perspective that remote sensing and its applications play a very important role in geological prospecting (Abdessamad El Atillah et al 2018). It thus considerably reduces the cost of exploration, by directing mining research towards favourable regions of a large area, which are sometimes inaccessible (Abdessamad El Atillah et al, 2018). For several years, remote sensing and airborne geophysical methods have been used to acquire data on the geological infrastructure of large areas (Rencz, 1999). Thus, multispectral (LANDSAT, ASTER, etc.), and hyperspectral (HYPERION, AVIRIS, etc.) imaging methods provide homogeneous and georeferenced coverage, of controlled resolution (quality of measurements, altitude, spacing) in very short acquisition, processing and archiving times. In the field of geology, the ASTER sensor remains one of the most widely used Earth observation satellites (Abdessamad El Atillah et al 2018). This sensor provides detailed information on the mineralogy and geochemistry of

\* Corresponding author: Daouda Illia Allo

rocks on the Earth's surface (Abdessamad El Atillah et al 2018). As part of this work, we use geomatics to direct our research towards areas potentially rich in iron ore. It will offer the opportunity to confirm field observations on geology and will also be a decision-making tool that will have the advantage of being economical, fast but above all applicable in remote and inaccessible areas. It is in this sense that we propose an integrated approach to digital processing of spatial data to respond to our problem while implementing modern analysis and modeling tools, hence the need for this bibliographic research. This work allows us to frame this theme in its scientific environment. The general objective of this work is to highlight the effectiveness of ASTER images in mapping areas with iron mineralization showings of the Continental Terminal 3 (Ct3) formation, southwestern part of the Iullemeden basin in Niger (Arewa region). Specifically, these are areas with major indices of iron oxides and hydroxides ( $\text{Fe}_2\text{O}_3 - \text{Fe}(\text{OH})_2$ ) and goethite  $\text{Fe}(\text{OH})_3$ .

## 2. Situation of the Iullemeden basin in its West African context

The Iullemeden Basin (named after the Tuareg confederation of the region) is a vast intracratonic basin in West Africa. It extends over more than 1000 km long, from north to south and over 800 km wide from east to west (Alzouma, 1994). Thus located, the Iullemeden basin communicates to the northwest with the Taoudeni basin via the Strait of Gao located between the Adrar des Iforas and the Gourma. It communicates to the east with the eastern Niger basin or Chad basin by the Dadermou threshold. Covering nearly 600,000 km<sup>2</sup>, the Iullemeden basin is surrounded by ante-ecbrian crystalline and crystallophyllian soils represented to the north by the Hoggar, the Adrar des Iforas and the Aïr, to the west by the Liptako basement in Burkina Faso and Niger, and to the south by the Benin-Nigerian Shield in Benin, Niger and Nigeria. The basin of the Iullemeden includes, in its northern part, the basin of Tamesna, Tim Mersoï, and Tin Seririne, and in its central part the plains of the Irhazer and Tegama. To the south, the Iullemeden basin is in continuity with the Kandi and Sokoto basins (Alzouma, 1994).

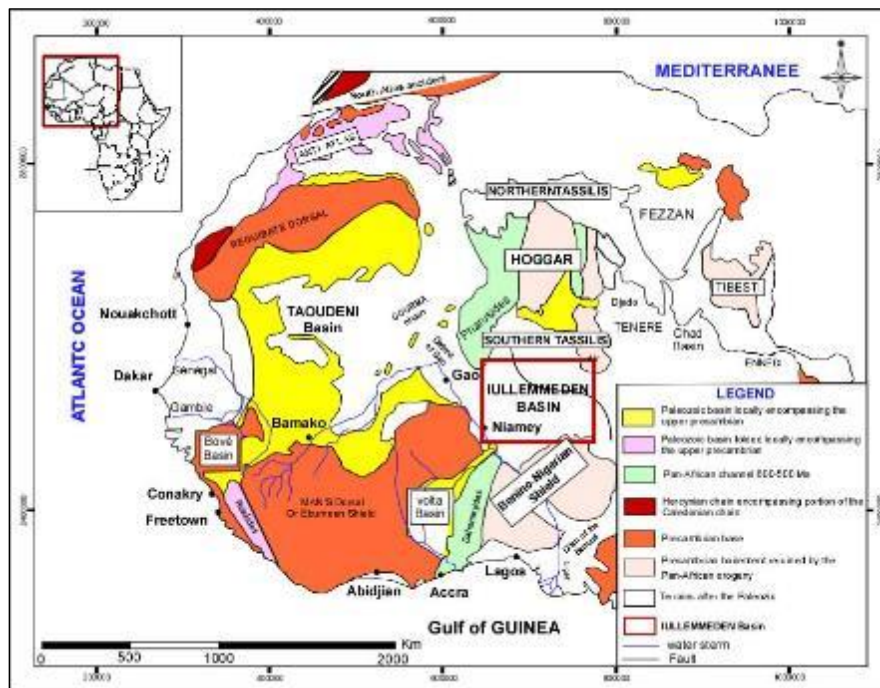


**Figure 1** Location map of the Iullemeden basin and the study area in West Africa (Trompette, 1973; modified).

## 3. Location of the study area in the context of the Iullemeden basin in Niger

In the western part of Niger, the Terminal Continental Formation represents the last series of fill deposits in the Iullemeden basin (Greigert, 1966). Indeed, Greigert (1966) defined three groups within this formation, from the bottom to the top: The Ader Doutchi siderolithic series (Ct1); the clay-sandy series with lignites (Ct2) and the series of clayey sandstones of the Middle Niger (Ct3). The Ct3 deposits subject to the present study, consisting of alternating clayey sandstones and ferruginous oolitic sandstones with indurated levels, lie in major unconformity on Neoproterozoic deposits and/or on the Paleoproterozoic (or Birimian) basement in the Niamey region (Hamza Mayaki et al., 2017; Ousmane et al., 2020).

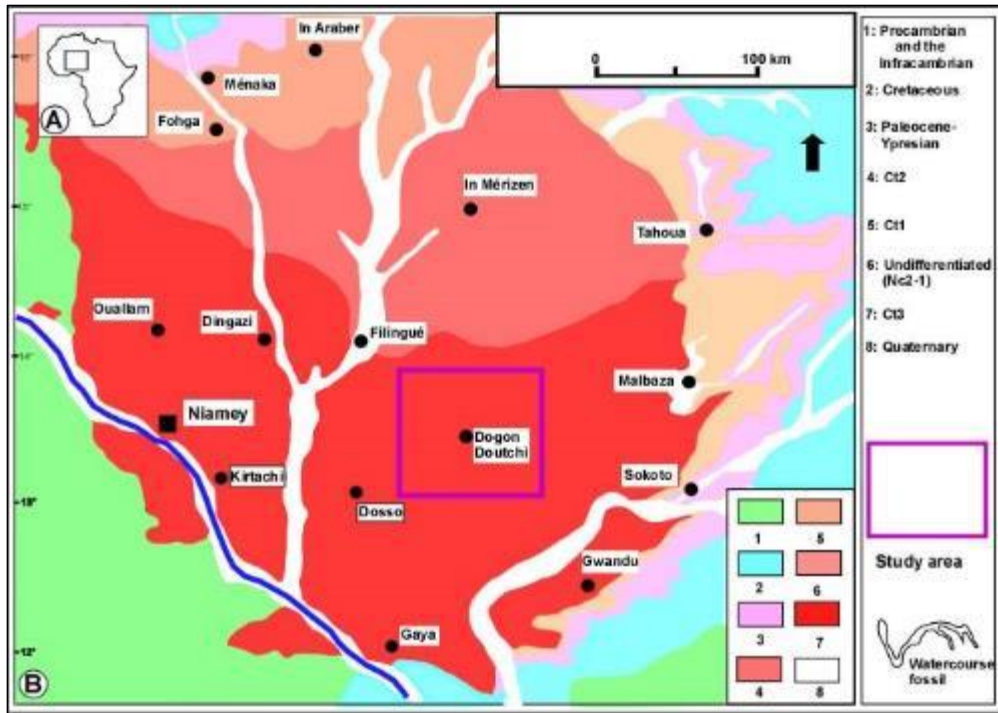


**Figure 2** Location of the Niger on the map of Africa; B: Geology of the Iullemmenden Basin (Greigert et Pougnet, 1965).

## 4. Material and methods

### 4.1. . Equipment

As part of his work, ASTER multispectral images were used for the mapping of iron ore-rich areas of metallogenic interest of the Terminal Continental 3 (Ct3) formation of the Arewa region.

#### ❖ ASTER Data

The ASTER image used in this study is a AST\_L1T with total absence of clouds. Acquired on December 9, 2023, it has been corrected, atmospheric effects and geometric distortions related to the sensor. The Aster image plays an important role in lithological discrimination. Table 1 gives a clear idea of the use of Aster strips for mineral exploration.

**Table 1** The different applications of ASTER images (Hamzaoui, 2005).

Bande (Aster)	Resolutions	Assemblage and alteration minerals
1, 2, 3	15 m	Hématite, jarosite, goethite, ferrihydrite
5 (2.145 – 2.185 µm)	30 m	Kaolinite, dickite, alunite, zunyite, topaz, jarosite, Pyrophyllite
6 (2.185 – 2.225 µm)	30 m	Illite, muscovite, smectite, jarosite
7 (2.235 – 2.285 µm)	30 m	Chlorite, amphiboles, biotite, épidote, nontronite, jarosite, dolomite, serpentine, tourmaline
8 (2.295 – 2.365 µm)	30 m	Carbonates, serpentines, nontronite, saponite, chlorite, amphiboles, biotite, épidote, tourmaline
9 (2.36 – 2.43 µm)	30 m	Chlorite, amphiboles, biotite, épidote, tourmaline nontronite, saponite

Mid-infrared and thermal infrared (Figure 3). The spatial resolution varies with wavelength: 15 m in the visible and near-infrared (VNIR-Visible and Near Infrared), 30 m in the mid-infrared (SWIR-Short Wave Infrared) and 90 m in the thermal infrared (TIR-Thermal Infrared).

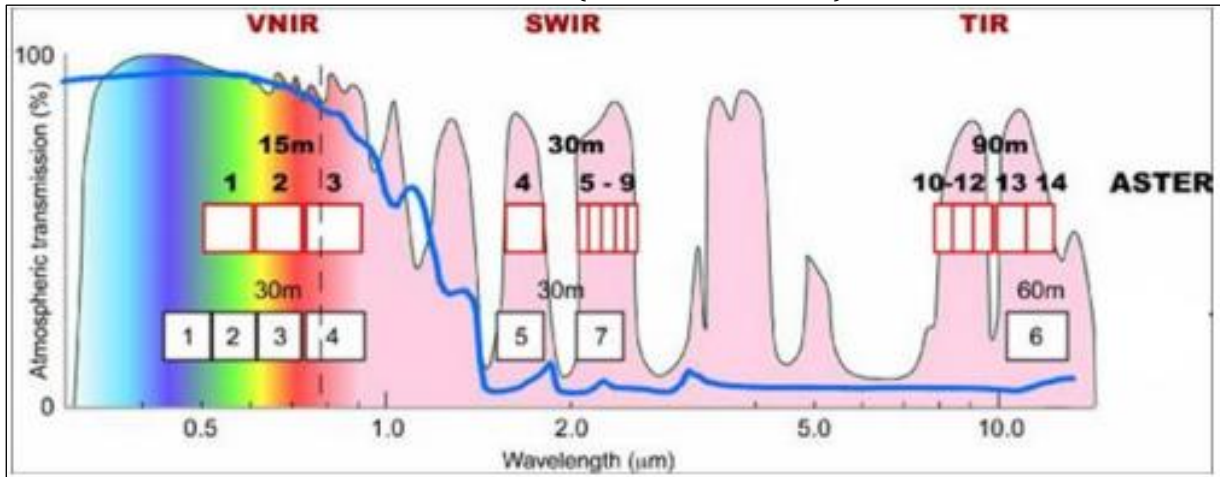


**Figure 3** Location of the 14 spectral bands of ASTER and on the atmospheric transmittance spectrum.

#### 4.2. Methodological approach

In the framework of this study, the following methodological approach has been adapted :

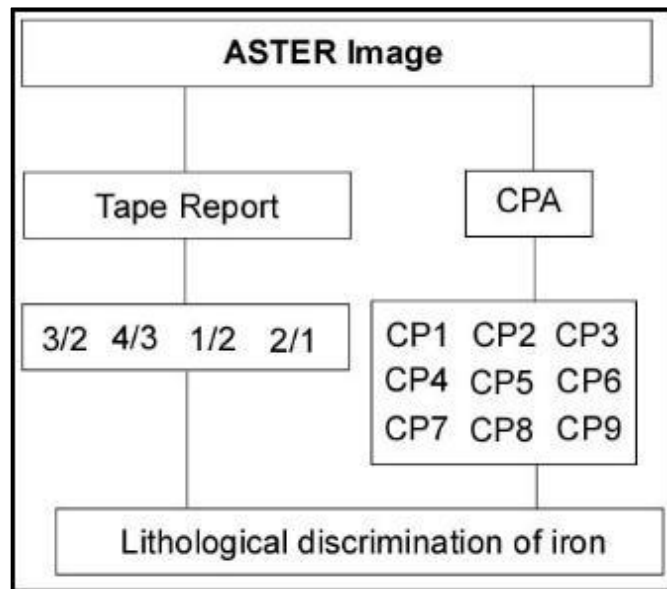


**Figure 4** Methodology approach

### 5. Result

#### 5.1. Principal Component Analysis (PCA)

The processing of the Aster image by Principal Component Analysis (PCA) allowed us to obtain nine (09) main components denoted CP1 to CP9, the results of which are presented in the table and figure below.



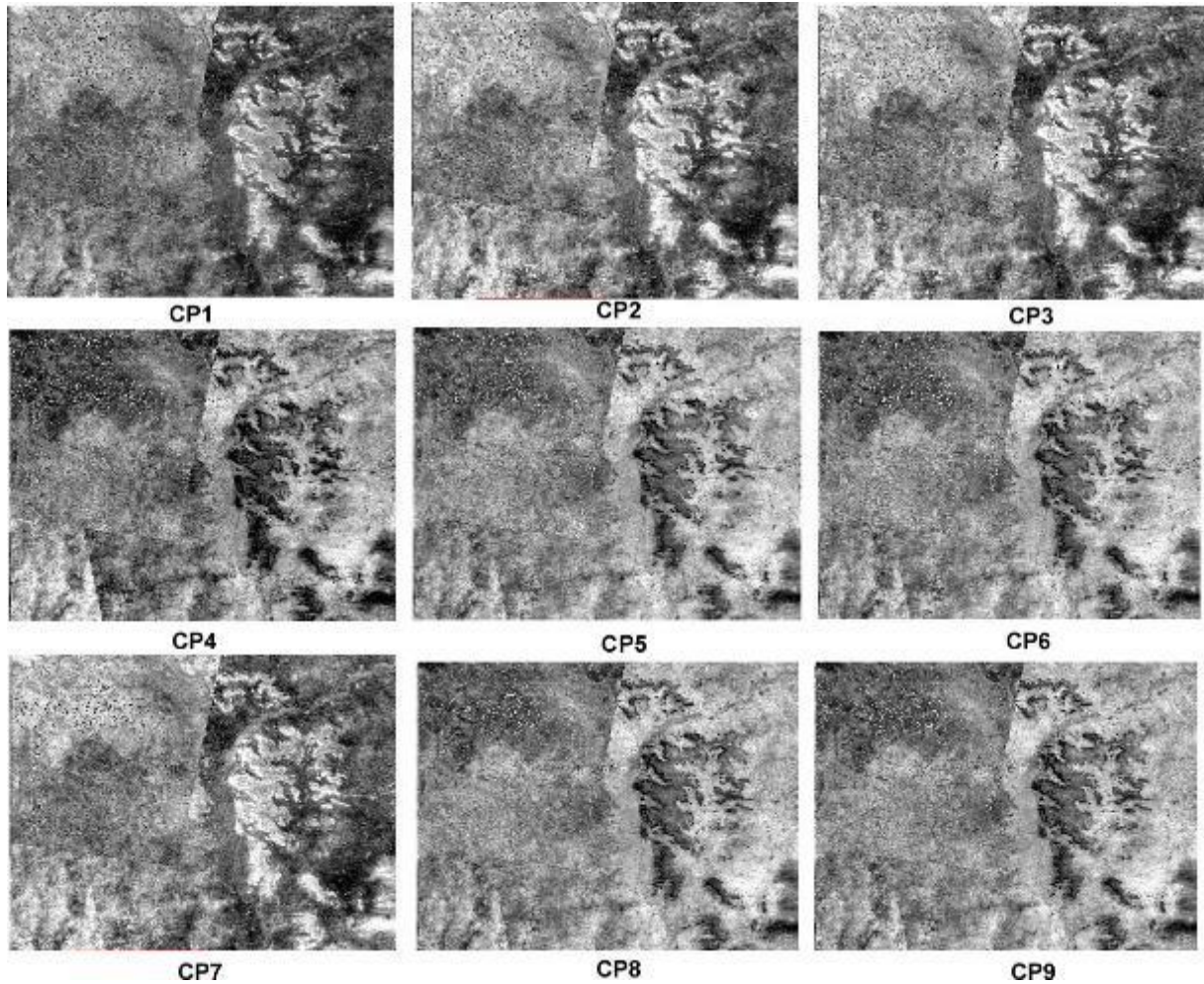


Figure 5 CPA result

Table 2 Eigenvector matrix from principal component analysis

	Band 1	Band 2	Band 3	Band 4	Band 5	Band 6	Band 7	Band 8	Band 9
CP 1	0,749	-0,171	0,2698	-0,1004	-0,1262	0,259	-0,512	-0,044	0,931
CP 2	-0,167	-0,4348	-0,418	-0,1018	0,1809	-0,1254	0,048	-0,525	0,1334
CP 3	0,2433	0,9355	-0,1621	0,1746	0,2463	-0,81	-0,1427	-0,66	0,207
CP 4	0,282	-0,066	-0,2957	0,3267	-0,036	0,229	0,521	-0,667	0,1685
CP 5	-0,3082	0,439	0,1747	-0,1801	-0,1479	0,597	0,1636	0,681	0,1105
CP 6	0,1304	-0,929	-0,2978	-0,404	0,2359	-0,2037	-0,1495	-0,295	0,2559
CP 7	0,76	-0,396	0,4377	-0,451	-0,1366	-0,228	-0,099	-0,814	0,1471
CP 8	-0,3092	0,6665	0,2043	-0,892	-0,2093	0,1759	-0,165	0,0347	0,264
CP 9	-0,1887	-0,066	0,2074	-0,1113	-0,55	0,555	0,576	-0,375	-0,0036

The analysis of its results of the nine (09) main components allows us to distinguish two predominant colors, the light color and the dark color. According to Velosky et al., 2003, the contributions of Aster bands 1, 2 and 4 in CP3 predict the presence of iron oxide distinguished by bright pixels because iron oxide has minimal reflectance in the visible range (Aster bands 1 and 2) and high reflectance in the near-infrared (band 4). The main components CP1, CP2, CP7 have the

same characteristics as the main component CP3. On the latter, a concentration of bright pixels can be observed at the outcrops of the terminal continental 3 of the study area.

## 5.2 Aster band ratios and indices

This method is based on the ratio of the bands. To highlight the lithological characteristics of the Iron, the ratios of Band 3 / Band 2, Band 2 / Band 1 / Band 1 were applied to the ASTER image of the study area, the result obtained following the processing of the images is presented in the figure below.

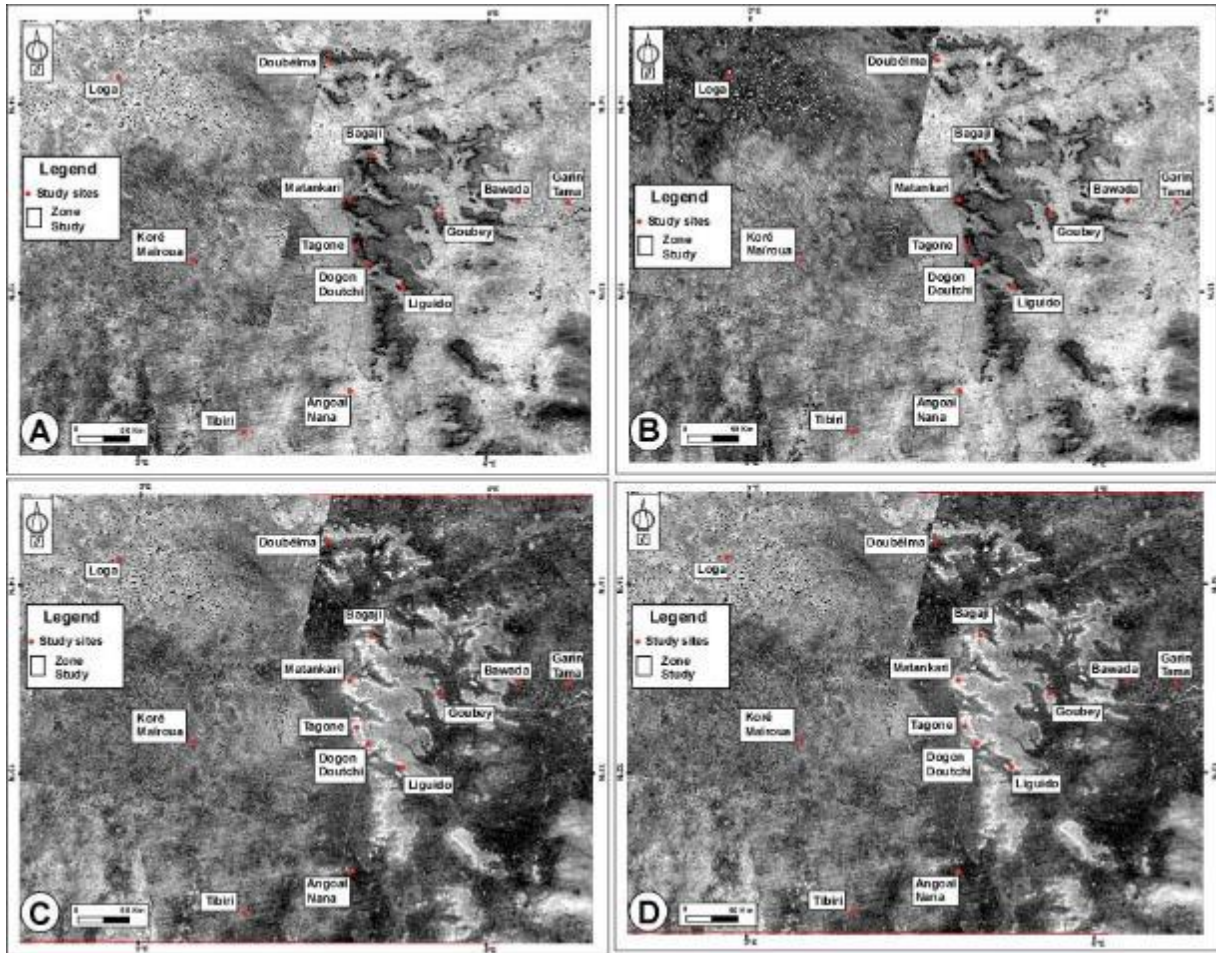


**Figure 6** Results of the band ratios on the ASTER A image: 3/2; B: 3/4; C: 1/2; D: 2/1

Rowan et al (2005) and El Qayedi et al (2006) used the ratio (Band 1 / Band 2) for the detection of ferrous iron ( $\text{Fe}^{2+}$ ). This ratio was applied to the ASTER image of the study area after masking the vegetation to eliminate its absorption effect in band 2. The ratio (Band 2 / Band 1) was used by Rowan et al (2003) to show the pixel distribution with intense absorption of ferric iron ( $\text{Fe}^{3+}$ ). Rouskov et al, (2005) used the ratio (Band 4/ Band 3), (also mentioned by Kalinowski et al, (2004)), to map the iron distribution, the use of this ratio (Band 2 / Band 1 and Band 1 / Band 2) on the ASTER image of the study area shows high concentrations of iron oxides and hydroxides at the top of the Ct3 outcrops in this part of the Arewa region.



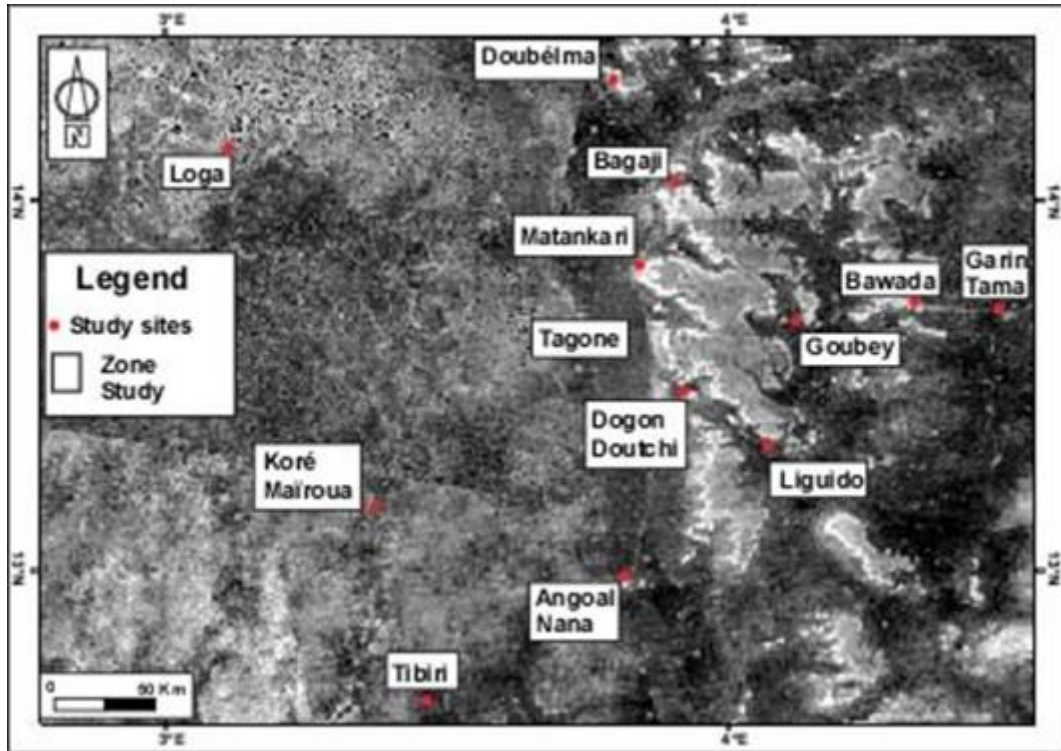


**Figure 7** Results of the band ratios on the ASTER image (1/2 - 2/1)

The RGB color composition of the 2:1 band ratios; 4+6/5; 3/2 (Figure 8), presents the outcrops of Ct3 by pixels in dark blue, these zones coincide perfectly with the tops of its outcrops of Ct3 occupied by a ferruginous armour, showing signs of iron mineralization.

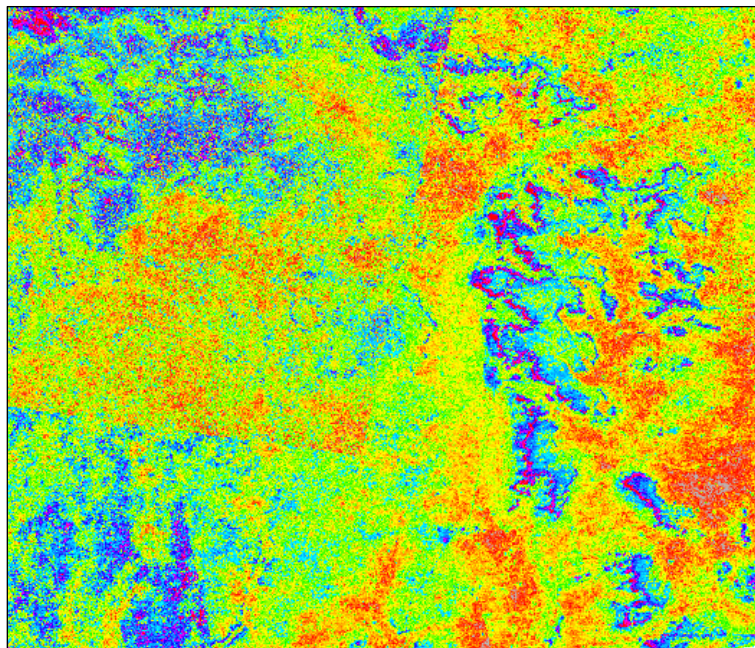


**Figure 8** the RGB color composition of the 2:1 band ratios; 4+6/5 ; 3/2.

In the Iullemeden and Kandi basins, the plateaus and mounds of the Terminal Continental frequently have a ferruginous armour at their summits with a mostly oolitic structure (Kamal, 2020). This tabular armoured level has been generally considered to be a particular aspect of laterite (Tessier, 1954). Various observations and studies, particularly microscopic studies, show that these are deposits of syngenetic ferruginous oolites, probably of lacustrine

origin, which must be clearly dissociated from the true laterites proper (Tessier, 1954). This area, characterized by a steep slope, is less conducive to vegetation growth, resulting in improved reflectance of the rocks. Figure (9) shows the different facies observed according to the south-north synoptic section. The latter shows the top of Ct3 in the study area is occupied by a more or less oolitic ferruginous armour. These observations are in agreement with Aster satellite data which distinguish the top of the Ct3 outcrops with clear pixels attributed to some authors to the presence of iron oxides and iron hydroxides.

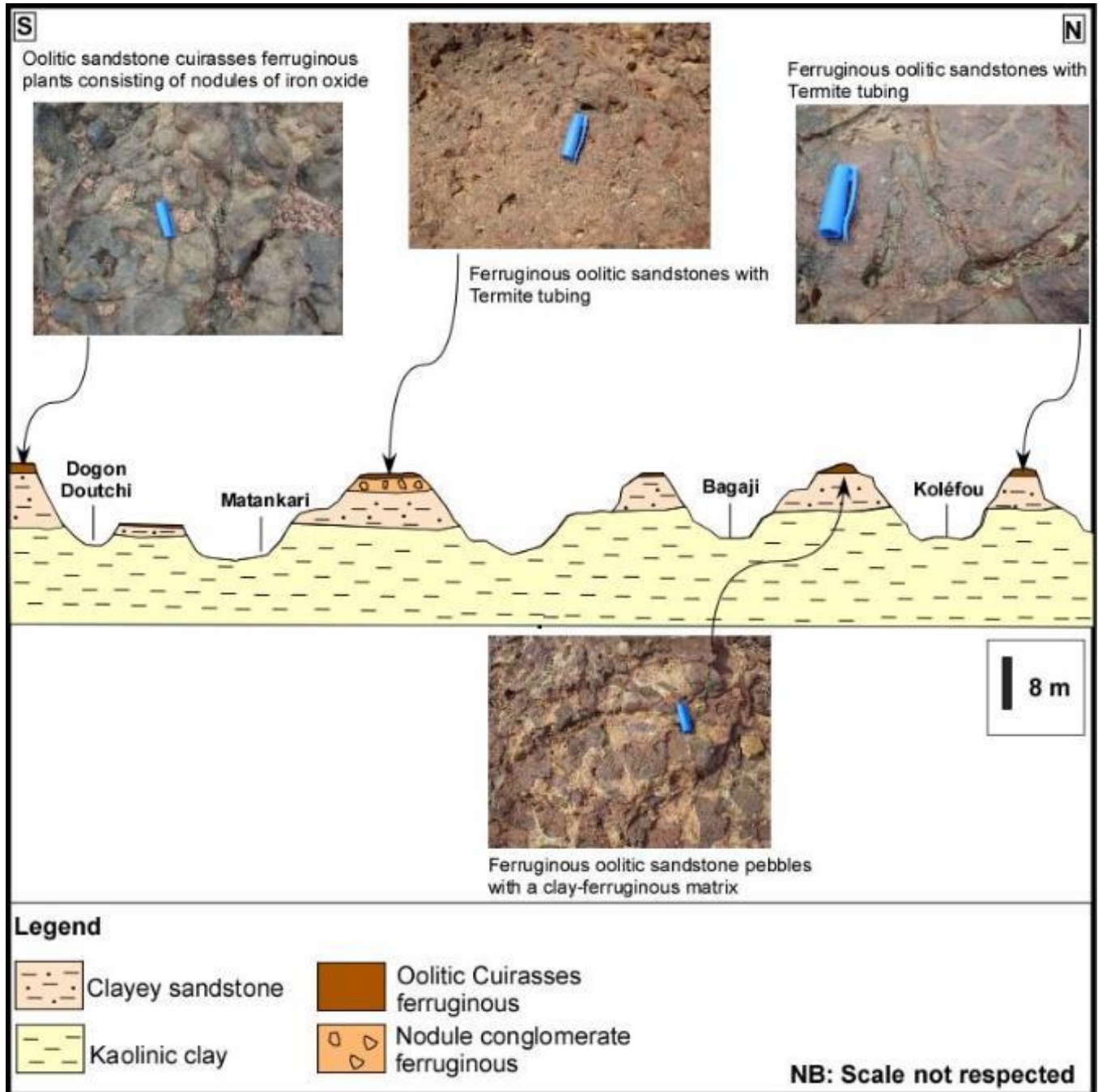


Figure 9 Synoptic section of the study area in the south-north direction

## 6. Conclusion

The study found that Band Reports, Band Indices and Principal Component Analysis (PCA) applied to ASTERS images have made it possible to detect and map anomalies related to the presence of iron in the Continental Terminal 3



formation of the Arewa region. The results obtained were effective and in line with the real conditions on the ground. These very interesting results have helped to complement the work carried out in the field.

---

## Compliance with ethical standards

### *Disclosure of conflict of interest*

No conflict of interest to be disclosed

---

## References

- [1] Alzouma k. (1994). Fluctuations in sea level during the mesozoic and cenozoic periods in the intracratonic iullemmeden basin (niger, west africa). *Biochronology and dynamics of sedimentary bodies. Africa geosciences review*, vol. L, n°2/3, pp. 131-281
- [2] Abdessamad el atillah, zine el abidine el morjani and mustapha souhassou, (2018), use of multispectral image for the exploration and research of mineral resources: state of knowledge and proposal of a processing model, 29p.
- [3] Fatiou a. K., (2020). Sedimentological, paleontological, paleogeographic and structural studies of maastrichtian to ypresian deposits in the iullemmeden basin (central niger). Ph.d. Thesis, abdou moumouni university of niamey. 237 p
- [4] Greigert j., (1966). Description of the cretaceous and tertiary formations of the iullemmeden basin (west africa). *Pub. Dir. Min. géol. Niger, n°2. Mém. B.r.g.m., n°36, 234 p.*
- [5] Greigert j., pougnet r., (1967). *Essai de description des formations géologiques de la république du niger.* Publication direction des mines et de la géologie, niger, n°3, 273 p.
- [6] Hamza mayaki i., souley h. And konate m. (2017). Geological and geotechnical characteristics of two geomaterials quarried in the niamey region: iron oolitic sandstones
- [7] Hamzaoui a. (23-25 november 2005): multispectral and hyperspectral remote sensing applied to mineral exploration. National days of the mineral industry., marrakech.
- [8] El qayed j., k. Taj-eddine, f. Bonn, m. Chikhaoui, o witam. Lithological characterization of the moroccan high atlas using aster data and spectral field measurements. *Remote sensing*, 2006, vol. 6, no. 2, p. 153-175.
- [9] Ousmane, h., dia h., k. Hamidou, l. B., ali, i. A., & konaté, m. (2020). Caractérisation de la déformation des dépôts oligocènes du continental terminal 3 (ct3) dans la région de niamey (bordure orientale du craton ouest africain, bassin des iullemmeden),24p.
- [10] Rowan. Lc., march. Jc., and simpson. Cj., (2005) lithologic mapping of the mordor, nt, australia ultramafic complex using the advanced spaceborne thermal emission and reflection radiometer (aster). *Remote sensing of environment*, vol. 99, pp. 105-126.
- [11] Rencz, andrew n., (1999) *remote sensing for the earth sciences - manual of remote sensing (3rd edition) volume 3.*
- [12] Trompette r., 1973. The upper precambrian and lower paleozoic of the adrar des mauritania (western edge of the taoudeni basin, west africa). An example of craton sedimentation. *Stratigraphic and sedimentological study.* - trav. Lab. Sci. Terre, marseille (st- jérôme), 1 and 2, 573 p.
- [13] Tessier f., (1954). Ferruginous ooliths and false laterites in the east of french west africa. Extract from the *annals of the higher school of sciences, institut des hautes études de dakar*, 26 p.
- [14] Velosky jc, stern rj, johnson pr (2003). Geological control of massive sulfide mineralization in the neoproterozoic wadi bidah shear zone, southwestern saudi arabia, inferences from orbital remote sensing and field studies. *Precam. Res.*, 123(2–4): 235–247.